

Propulsion System for Hypersonic Space Planes

Michael Zeutzius,^{*} Toshiaki Setoguchi,[†] Kunio Terao,[‡] and Hideo Miyanishi[§]
Saga University, Honjo, Saga 840-8502, Japan

Because of its simple construction and low weight, combined rocket, ramjet, pulse-jet engines, or detonation engines instead of turbojets, were taken into consideration as propulsion for hypersonic aircraft. Combined propulsion requires an active control system to change the propulsion operation mode and to sustain the high-efficient pulse combustion. Therefore, the transient behavior of the combustor is investigated to show the benefits that can be gained, especially from a pulse combustor with active control. Several experiments were performed to survey system performance and to find suitable control parameters and strategies. Propulsion installation, including thrust augmentation, is considered to define the tasks of the combustor controller.

Nomenclature

A	= cross section
b	= fuel consumption
c	= sound velocity
D	= pipe diameter
F	= thrust
f	= frequency
H	= net calorific value
L	= tail pipe length
M	= Mach number
\dot{m}	= mass flow
n	= rotational speed
P	= pressure
Re	= Reynolds number
T	= temperature
t	= time
u	= velocity
X, Y	= coordinates
α	= angle of attack
ΔP	= pressure amplitude
η	= efficiency
κ	= ratio of specific heats
ρ	= density

Subscripts and Superscripts

A	= air
C	= combustion chamber
E	= settling chamber
F	= fuel
H	= high pressure (>100 kPa)
i	= inlet
L	= low pressure (<100 kPa)
N	= nozzle
set	= set value
th	= thermal
V	= propulsive efficiency
0	= stagnation
∞	= ambient
'	= periodic perturbation
-	= mean

Introduction

ALTHOUGH during the last decade much effort has gone into the development of space planes, general interest in space plane technology is declining, and most projects have already stopped. Nevertheless, there are actual activities that concentrate on the development of propulsion for a future space plane¹ or hypersonic aircraft. Although experimental and numerical results of research on components and proposals for a possible steady flow propulsion^{2,3} and combined propulsion,⁴ including propulsion installation,⁵ are sufficiently available in the open literature, there is minimal work that deals with nonsteady flow engines. Here, the feasibility of running a single combustor as pulse, ram, or rocket propulsion is discussed.

The basic physics of pulse combustion are reported in contemporary literature.^{6,7} As current experiments show, pulse combustors with an active control system provide significant higher performance than conventional combustors with a fixed geometry. Therefore, this paper deals with the design of combustor control devices and an investigation of the efficiency of several possible control strategies. The investigation includes an analysis of the transient behavior of the control devices to accomplish the required operation modes with only one combustion chamber. How to sustain higher thermal efficiency of pulse combustion for high flight velocities considering propulsion installation is also discussed.

Propulsion Concept

With combined propulsion, the turbojet runs only during the start and the acceleration phase; therefore, it is desirable to find suitable start-capable propulsion without a turbojet. The weight of a turbojet, for example, for a two stage to orbit system, is quite high and amounts to one-third of the total takeoff weight. In addition, the demand for undistorted flow that has to be supplied to the compressor, the installation integration into a space plane, and the different cross section of the two-dimensional inlet and the turbojet necessary for the required operational flexibility complicate the construction of an appropriate turbojet engine. The combination of a rocket, pulse, and ram-/scramjet becomes very attractive because of simplicity and possible low-cost manufacturing.

Here combined propulsion means the parallel operation of different propulsion types, as well as the operation of one combustor in different modes. The controller is not only required for changing the operation mode, but is also necessary to make full use of the performance of pulse combustion. The basic control idea is shown in Fig. 1. The controller defines the most efficient operation mode, depending on the combustor state and the power demand of propulsion and aircraft, respectively. The set values for the flow rates were taken from an experimentally obtained fuel-performance map governing the nonlinear characteristics of the combustor that are at present not possible to calculate. The main purpose of present investigation is to carry out the transient behavior of the combustor, especially the fuel-performance map.

Received 30 March 1998; presented as Paper 98-1531 at the AIAA 8th International Space Planes and Hypersonic Systems and Technologies Conference, Norfolk, VA, 27–30 April 1998; revision received 19 February 1999; accepted for publication 25 February 1999. Copyright © 1999 by the American Institute of Aeronautics and Astronautics, Inc. All rights reserved.

^{*}Associate Professor, Department of Mechanical Engineering.

[†]Professor, Department of Mechanical Engineering.

[‡]Professor Emeritus, Department of Mechanical Engineering.

[§]Graduate Student, Department of Mechanical Engineering.

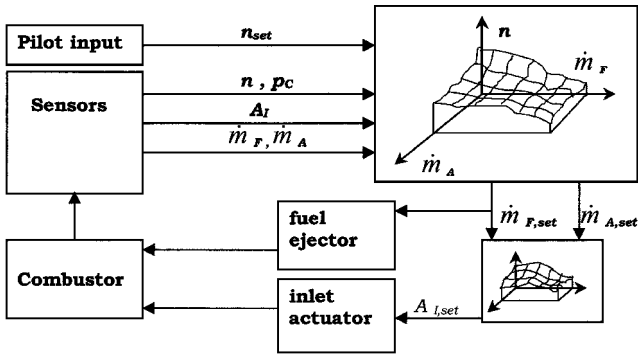


Fig. 1 Scheme of the control system.

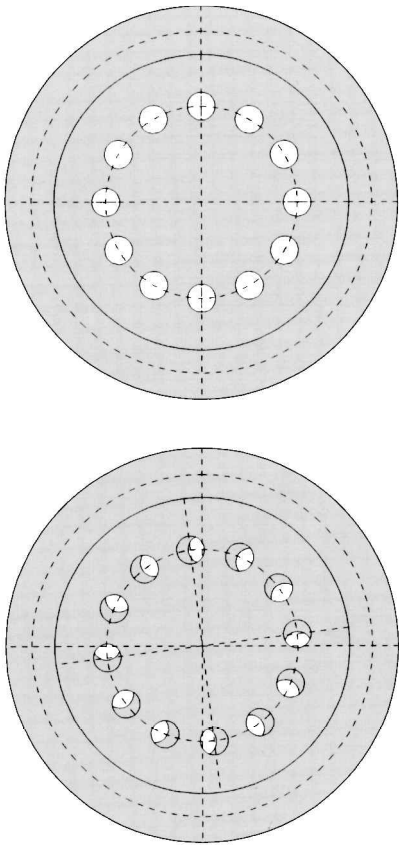


Fig. 2 Overlapped porous plates for flow rate control.

The control method itself is a kind of flow rate control with the inlet as the actuator. The inlet area of the two-dimensional version can be controlled with a movable ramp, and the inlet area of the axisymmetric combustor can be controlled with two overlapped porous plates, as shown in Fig. 2. Moving one plate against another changes the inlet throat cross section and the flow rate, respectively. For example, a ram-/scramjet can be operated as a rocket engine by fully closing the inlet and feeding oxygen from tanks into the combustion chamber. However, the rocket run time should be reduced to a minimum because this operation mode requires carrying an onboard oxidizer and increases the total weight. Throttled airflow through the inlet and the subsequent charge attenuation cause the pulse combustion mode.

Considering again the system installation into a space plane, there are multiple and sometimes conflicting requirements for an optimization. Whereas a choked inlet flow is necessary to sustain the pulse combustion and to improve the thrust under high subsonic flight conditions, the installation losses might increase due to a higher spillage rate than the one produced by a turbojet. The high

stagnation pressure at the inlet limited the operating range of past pulse-jet engines without active control devices. Excessive air rates entering the engine turned the pulse flow in steady flow (ram mode) so that the net thrust decreased. Concerning proposals for thrust augmentation, the reader is referred to Ref. 8 for a summary of several methods, whose feasibility is not yet shown experimentally. A version modified for space plane application with a boundary-layer bleeding system and thrust vector control (for details see Ref. 9) is shown in Fig. 3. The propulsion can be operated in the following modes: 1) combined pulse/rocket mode during takeoff, 2) pulse mode at subsonic flight speeds, 3) ram/rocket mode during transonic flight, 4) ram/scram mode during supersonic flight, and 5) rocket mode at high altitude or space flight.

Experimental Setup

A parameter variation of the combustor geometry has shown that the flow rates have the strongest influence on combustor operation and performance. Therefore, the flow rates and the inlet cross section, respectively, were chosen as control parameters. The two-dimensional version of the combustor equipped with a movable inlet ramp to adjust the inlet cross section is shown Fig. 4a. The combustor performance was measured with an impulsive turbine located at the nozzle exit for varying fuel flow rates and inlet cross section. The combustor characteristics comprise the fuel-performance map or semiempirical relationships, for instance, higher-order series, whose accuracy is fully sufficient to design a controller algorithm.

The goal is a so-called closed-loop run, which operates the combustor with an inlet cross section controlled by a motor sensing pressures and energy demand. The energy demand is calculated based on the actual rotational speed of the turbine. The turbine is connected to a generator, and the rotational speed is derived from the generated voltage signal. The pressure was measured with water-cooled piezometric pressure transducer that has an accuracy of 2% dependent on temperature effects. The inlet damping chamber, as shown in Fig. 4a, is only used to measure the airflow rate. It is not a part of the propulsion.

The whole ejector system is installed in front of the inlet for better ejector adjustment. Additional air ejection improves the vaporization and mixing. Air ejection and ignition with a spark plug are required for the start of the pulse-jet combustor.

Concerning propulsion installation, the external flow around the propulsion is simulated with the Eiffel-type wind tunnel of Saga University (Fig. 4b) with an open test section. Start and takeoff conditions can be simulated with a maximum freestream velocity of $u_\infty = 35$ m/s. The velocities are calculated from measured pressure data for incompressible flow. The engine (length 80 cm, pipe diameter 34 mm) was set in the wind tunnel with a pendulum suspension so that the forces can be obtained from the engine displacement.

Results and Discussion

Wind-Tunnel Test

These experiments were performed to investigate the reason for the limited operating range of past pulse-jet engines and to define the tasks of the control system. The overall net performance depends on thrust and spillage drag. Spilling airflow at the inlet can be seen from the flowfield shown in Fig. 5a for a pulse-jet engine with an aerovalve. The freestream velocity of 24.8 m/s is reduced to 14.3 m/s in front of the inlet resulting in a spilling air rate $\Delta \dot{m}_\infty$ in the order of magnitude of about 40% as estimated by the following equation for incompressible steady flow:

$$\Delta \dot{m}_\infty / \dot{m}_\infty = (u - u_\infty) / u_\infty \tag{1}$$

A reversal of the inlet flow occurs if the combustion pressure exceeds the inlet stagnation pressure. This discharge of flue gas through the inlet causes thrust and inlet nonuniformity losses that can be calculated (after Busemann) with

$$\eta_V = 1 - \frac{1}{\dot{m} \bar{u}_N^2} \int u_N'^2 dm_N \quad \text{with} \quad u_N = \bar{u}_N + u_N' \tag{2}$$

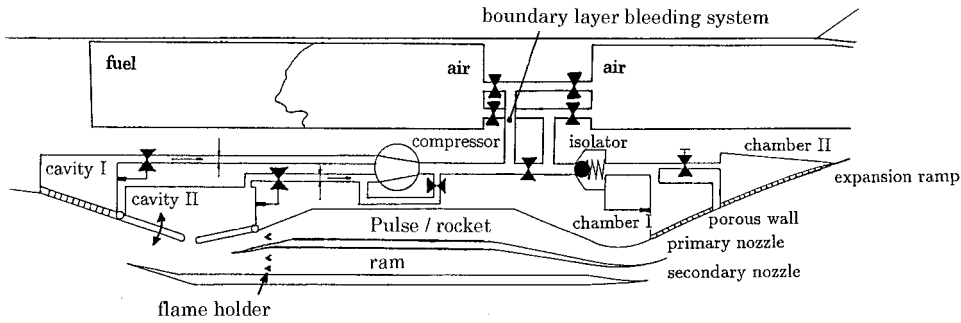


Fig. 3 Propulsion system installed into space plane.

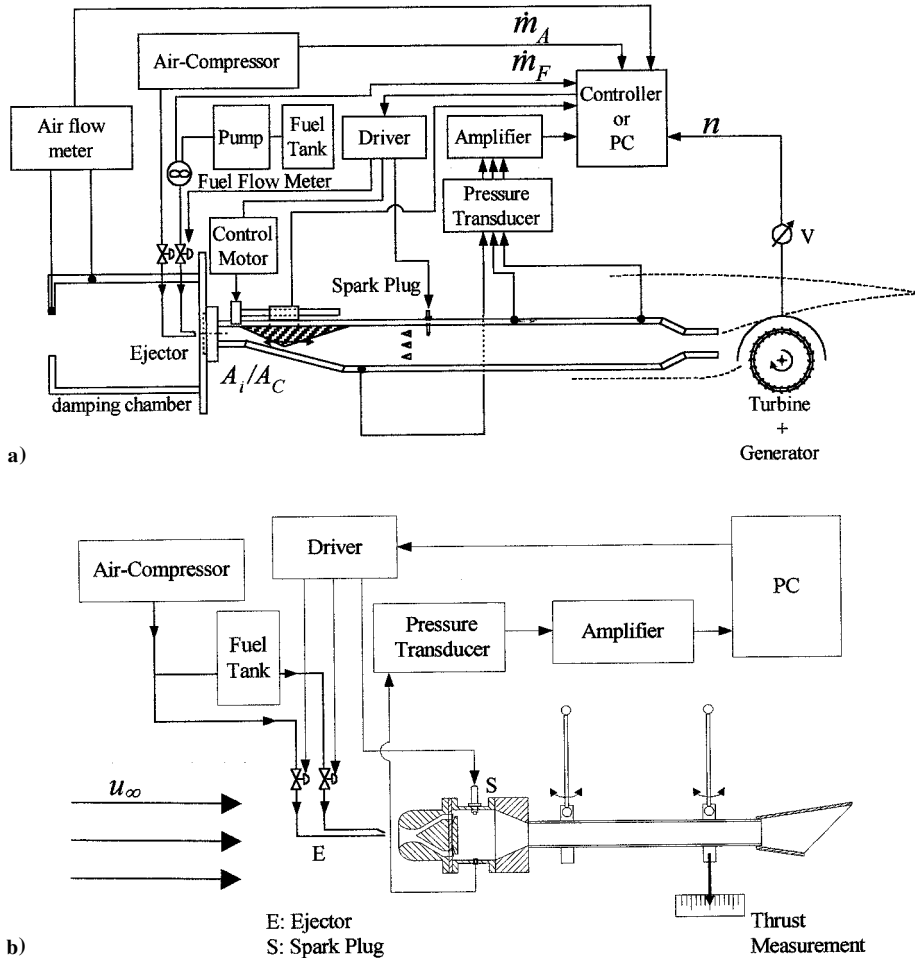


Fig. 4 Experimental setup: a) two-dimensional combustor with control system; control parameters: fuel rate and inlet cross section; controlled parameter: turbine speed; feedback parameters: pressures, flow rates, rotational speed of the turbine, and cross section and b) wind tunnel, with axisymmetric combustor.

and the thrust with

$$F = \dot{m}_N(\bar{u}_N - u_\infty) = \dot{m}_N \left[\sqrt{\eta_V (2\eta_{th} \dot{m}_F H + u_\infty^2)} - u_\infty \right] \quad (3)$$

The flow rates and the exit velocity of the burned gases could not be measured in the wind-tunnel experiment, but the mean velocity was estimated to be about 200 m/s (Ref. 10). The thrust and drag generated by the small-scale engine are shown in Fig. 5b. The drag of the basic engine is quite high. By redesigning the nacelle, the drag could be reduced by one-half. With a high integration into the inlet ramp, as proposed in Fig. 3, further reduction of the drag can be expected.

The thrust itself depends on the inlet valve system. The ram thrust is caused by the fuel–air–ejector system (similar to an ejector pump) and is fully negligible for low-speed flight. Higher thrust is obtained

for aerovall engines by slightly increasing the stagnation pressure over that which occurs due to increasing airflow rate. Engines with reed valves generate the highest thrust, but the rising stagnation pressure difference between inlet and nozzle reduces the combustion pressure amplitudes due to the high air inflow in the combustor, shown in Fig. 6. The pressure acting on the valve is too high for a rapid closing so that charge attenuation is too weak for a sufficient pressure drop in the combustor. As a result, the pressure amplitudes decrease with increasing stagnation pressure, and the flow through the combustor gradually approaches the steady flow (ram mode) with a lower thermal efficiency (constant pressure combustion). The combustion mode depends strongly on A_i/V_i and A_N/V_N due to its strong impact on charge and discharge time.¹¹ An active control of the inlet cross section or an adjustment of the nozzle exit pressure by a secondary jet prevents the undesired change of the operation mode.

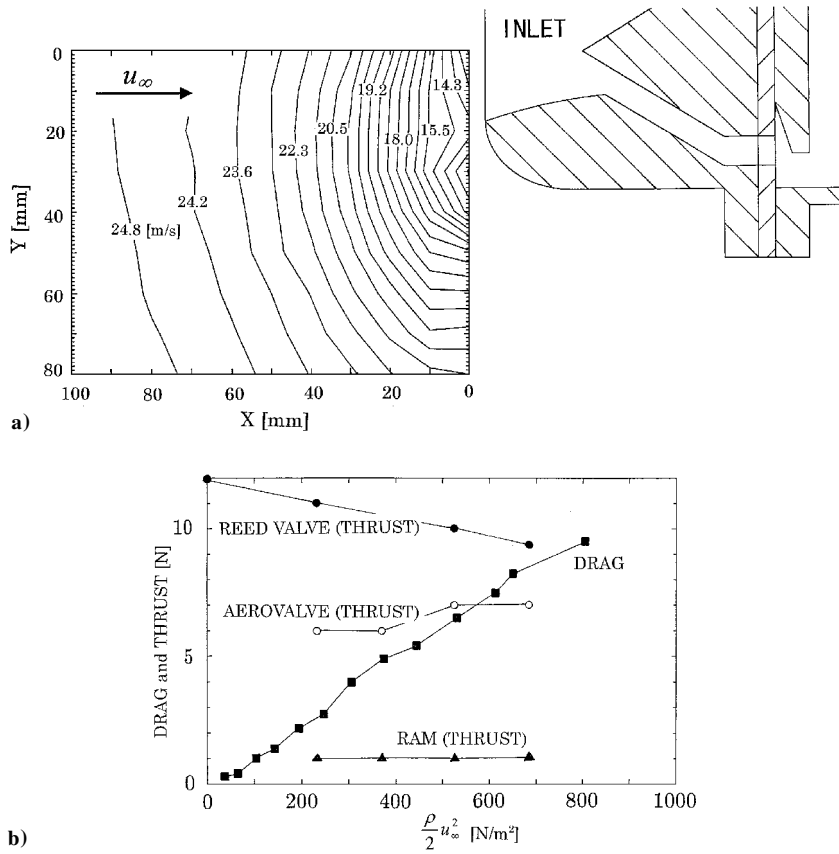


Fig. 5 Pulse-jet engine: a) velocity distribution in front of the inlet (spillage) and b) drag and thrust depending on operation mode.

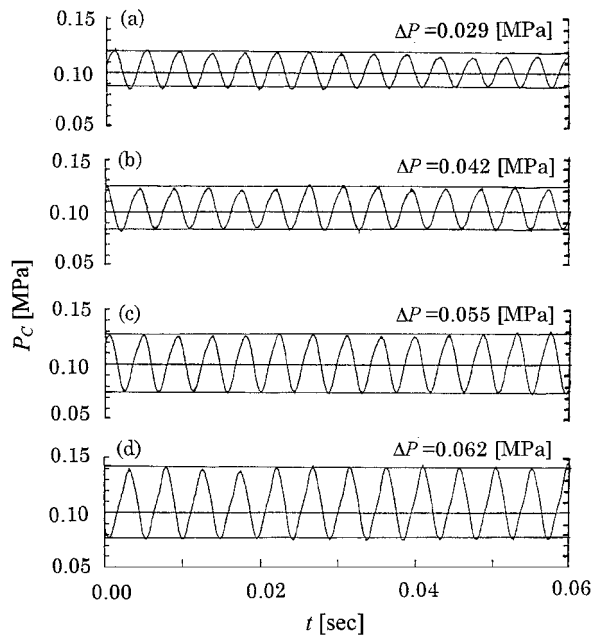


Fig. 6 Combustion pressure amplitude dependent on flight velocity: a) $u_\infty = 33.44$ m/s, b) $u_\infty = 29.02$ m/s, c) $u_\infty = 24.51$ m/s, and d) $u_\infty = 19.42$ m/s.

In a summary, it is the task of the controller to keep the combustion pressure amplitude and flow rates as high as possible.

Thrust Augmentation and Nozzle Integration

The experiments were performed at an atmospheric pressure that is very low for propulsion application. However, high combustion pressure amplitudes and thrust augmentation gained with symmetric nozzles are also obtained for asymmetric external nozzles, which are necessary to reduce the base drag. The history of the combustion

pressure shows that not only higher pressure amplitudes were obtained for asymmetric nozzles, but also detrimental high-frequency pressure oscillations (Fig. 7a) as they occur in conical nozzles are avoided (Fig. 7b). These oscillations might have their origin in jet instabilities, overexpansion, and separation within the internal nozzle. The possible entrainment of ambient air in the external nozzle flow enables a natural damping of these oscillations.

Experiments have also shown that the total performance of the engine depends on the nozzle inclination. If the asymmetric nozzle is inclined so that the upper wall is aligned to the pipe (Fig. 7c), the thrust decreases to the same value as an engine with a straight tailpipe. It is fortunate that the nozzle type suitable for an integration with lowest base drag delivers the highest thrust. The mean pressure increases from 107 to 112 kPa and results in a considerable thrust augmentation for atmospheric combustion.

Engine in Parallel

Several parallel engines have to be installed into a space plane. The functionality of a twin system is explained here in detail because the twin pulse combustor as gas generator can possibly replace conventional combustion chambers in a turbojet to gain higher thermal efficiency. As shown in Fig. 8, the gas column oscillating with a frequency of about 300 Hz compresses the mixture that is charged through the inlet. The excess gas from combustor B that cannot enter the pipe leaves the combustor through the silencer chamber. The combustion further raises the pressure in chamber A (Fig. 8a), and the subsequent pressure waves propagating through the pipes compress the mixture in combustor B (Fig. 8b). The inertia of the burned gases in the tailpipe lowers the pressure in combustor A, so that fresh air can enter the combustor, and the next cycle starts.

Coupled engines with a common inlet and nozzle operated in antiphase (Figs. 8c) enable a constant volume combustion (pulse mode) and a steady flow leaving the engine, as shown in Fig. 8d. To keep the nonuniformity losses as low as possible, the flow should leave the nozzle with a constant velocity. The thrust of a combined

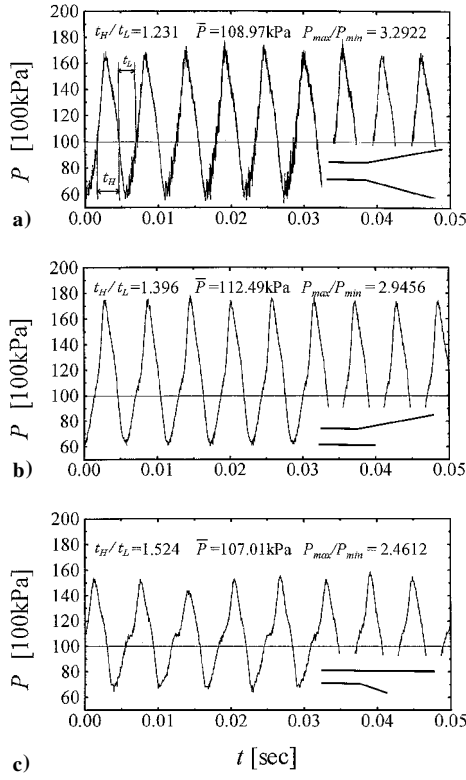


Fig. 7 Installation of asymmetric nozzles, operated in pulse mode: a) conical nozzle, b) asymmetric, nozzle lower side wall aligned to centerline, and c) asymmetric nozzle, upper side wall aligned to centerline.

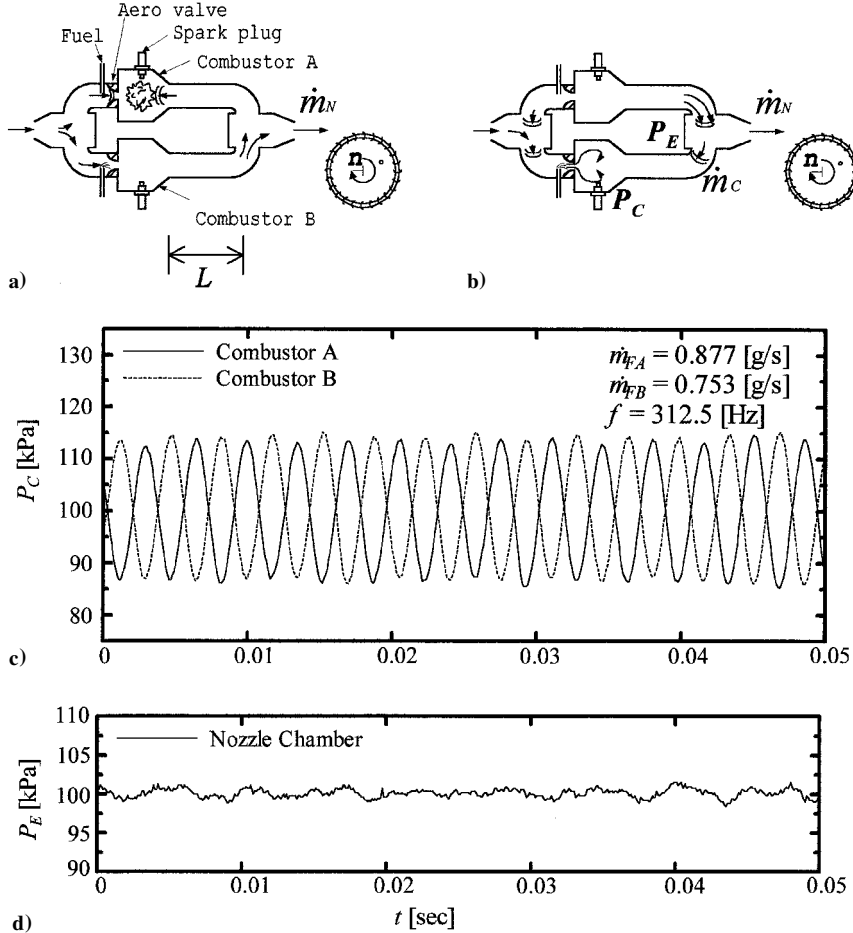


Fig. 8 Working principle of twin combustor: a) raising pressure in chamber A, b) compressing mixture in chamber B, c) history of the combustion pressure, and d) history of the settling pressure.

engine is slightly lower than the sum of the thrust that each engine would generate individually due to a reduced air rate leaving the combustor. A certain amount of the gas accelerated by one combustor is used for the compression of the fresh mixture in the second combustor. The excess gas that cannot enter the second pipe is leaving the propulsion. Therefore, \dot{m}_N represents the effective flow through the combustor. The tailpipe length is the related parameter governing friction losses and compression capacity due to the inertia of the accelerated gas. The reduced total pumping capacity¹² \dot{m}_N (Fig. 9a) for a short tailpipe ($L/D = 4.8$) causes thrust losses or a reduction of the kinetic energy of the burned gas, as can be seen from Figs. 9b and 9c, compared to combustors with a long tailpipe ($L/D = 10.4$) if the gas cannot be accelerated to higher speeds u_N . On the other hand, friction losses within the tailpipe reduce the pressure amplitude and the velocity for $L/D = 10.4$. An optimum could be found for a tailpipe with a length to diameter ratio of 7.6.

The rotational speed for the transferred energy shown in Fig. 9 for different pipe lengths shows the superiority of pulse combustion over steady combustion. Pulse combustion offers an enormous capacity for fuel savings. The rotational speed of the turbine shows that the energy output does not increase significantly with the fuel rate. Therefore, the highest efficiency is obtained for low fuel rates (E in Fig. 9c) and maximum power (M in Fig. 9c). As a result, the controller must optimize the flow rate ratio \dot{m}_C/\dot{m}_N for a high total efficiency and guarantee a stable antiphase run of both combustors.

Combustor Operation

Pulse combustion can also be seen as a kind of choked flow through the combustor or a flow with attenuated charge⁷ of fresh combustible mixture. This attenuation causes an oscillation of the gas column in the tailpipe that raises the burning rate and the combustion pressure due to the inertia of the flue gas in the tailpipe.

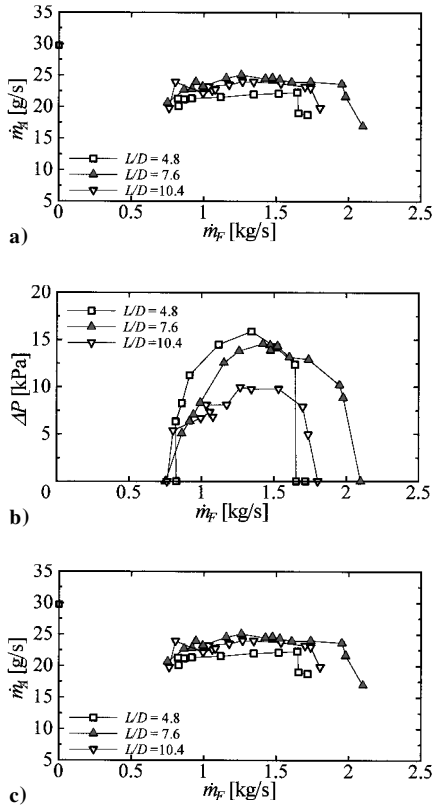


Fig. 9 Dependence on fuel rate and pipelength of: a) air rate, b) amplitude, and c) rotational speed of the turbine (kinetic energy of fuel gas).

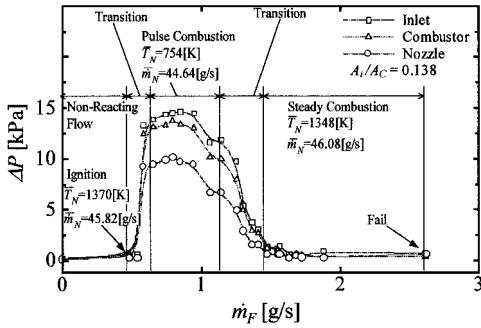


Fig. 10 Pressure history of a two-dimensional engine in inlet, combustor, and nozzle.

The combustion efficiency approaches that of the constant volume mode.

A characteristic pressure history of the two-dimensional combustor running in a pulse mode is shown in Fig. 10. After igniting, the pressure amplitude rises with increasing fuel rate within a small transition range to values of 15 kPa until the pulse combustion is established. Steady combustion is sustained for fuel rates higher than 1.5 g/s, and it is extinguished for fuel rates higher than 2.7 g/s. Aside from the fuel rate and ejection pressure, the combustor can also be controlled with the air rate and the inlet cross section, respectively. A simplified law for the combustor control can be linearized for a combustor run close to the design point in a first approach as

$$dn = \left(\frac{\partial n}{\partial \dot{m}_F} \right) d\dot{m}_F + \left(\frac{\partial n}{\partial \dot{m}_A} \right) d\dot{m}_A \quad \text{with} \quad (4)$$

$$d\dot{m}_A = \left(\frac{\partial \dot{m}_A}{\partial (A_i/A_C)} \right) d\left(\frac{A_i}{A_C} \right)$$

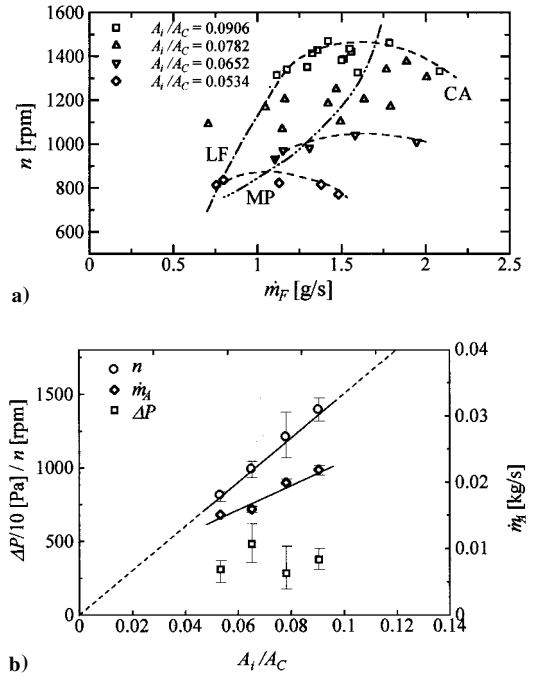


Fig. 11 Twin combustor: a) turbine performance dependent on \$\dot{m}_F\$ and b) air rate, amplitude, performance dependent on inlet cross section (overlapped porous plates).

The derivatives are obtained from experimental results, shown in Fig. 11. Unfortunately, fuel and air rate are not fully independent. Higher amplitudes for higher fuel rates reduces the airflow rate through the combustor. Assuming a nearly harmonic nozzle exit pressure, the nozzle exit velocity scales with the amplitude as

$$\bar{u}_N = (2/\pi) u_{\max} = (2/\pi) (c \Delta P / P_0 \kappa) \quad (5)$$

so that thrust and energy can be written as

$$F = \dot{m}_A (u_N - u_\infty) \sim \dot{m}_A \Delta P_C \quad (6a)$$

$$n \sim \dot{m}_A \Delta P_C^2 \quad (6b)$$

Because the pressure amplitude depends on fuel- and airflow rate, it is recommended to use the amplitude as basic parameter within the control system. The airflow rate can be calculated with the mass flow equation and the nozzle exit pressure P ,

$$\dot{m}_A = \rho A u = A \sqrt{2 P_C \rho C} \sqrt{\frac{\kappa}{\kappa - 1} \left[\left(\frac{P}{P_C} \right)^{2/\kappa} - \left(\frac{P}{P_C} \right)^{(\kappa + 1)/\kappa} \right]} \quad (7)$$

Basic features of pulse/steady combustion are reported in Ref. 13. Enhancing the fuel rate or opening the inlet turns a pulse flow into a steady one. In the application here, it is necessary to sustain the pulse combustion even for higher inlet stagnation pressures. Regarding Eq. (7), the air rate can be kept constant by reducing the inlet area.

The dependence of the kinetic energy of the burned gases on the inlet opening ratio and fuel rate is shown in Fig. 11a for a twin combustor with axisymmetric pipes. The fuel derivative $\partial n / \partial \dot{m}_F$ is fitted into a higher-order series for constant inlet cross section

$$\frac{\partial n}{\partial \dot{m}_F} = a_n \dot{m}_F^n + \dots + a_2 \dot{m}_F^2 + a_1 \dot{m}_F + a_0 \quad (8)$$

and must be determined for different cross sections. A simpler method to comprise the combustor characteristic is the mapping shown in Fig. 2 for a full-size combustor run. For the small-scale

test version, the power series is sufficient for a basic control algorithm design. The relation between the inlet opening ratio and turbine speed, the air rate, and the pressure amplitude is presented in Fig. 11b. The characteristic derivatives needed for control law Eq. (4) are

$$\frac{\partial n}{\partial (A_i/A_c)} = 15,300 \quad (9a)$$

$$\frac{\partial \dot{m}_A}{\partial (A_i/A_c)} = 0.256 \quad (9b)$$

These derivatives are only valid for one combustor geometry, which has a characteristic length ratio of $L/D = 5$. Maximum performance is obtained for the pulse mode with almost stoichiometric combustion, i.e., $\dot{m}_A/\dot{m}_F = 14.7$. Several possible control methods are shown in Fig. 11a. Constant area control (CA), i.e., only the fuel flow rate is controlled, is recommended for small deviations from the design operation. In general, for changes of combustor operating conditions, an adjustment of the inlet cross section must be included to sustain the pulse combustion. Maximum power (MP) and the most attractive lowest fuel consumption (LF) control include adjustment of air and fuel flow rate, as well. These operation conditions were derived from the CA-control data by just connecting the extrema.

The two-dimensional combustor shows similar characteristics of pumping capacity, with amplitude and turbine speed shown in Figs. 12a–12c. For low area ratios, the relation between turbine speed and fuel rate has a parabolic character. For higher ratios, the turbine speed remains almost constant due to the high airflow rate through the combustor. Figure 12c demonstrates the utility of a variable inlet for control and design of pulse combustors. The fuel consumption is reduced by half that of steady combustion. Whereas a low area ratio is beneficial for highly efficient combustion (E in Fig. 12c), it cannot be used for a mode change in a propulsion application by only controlling the fuel rate. The subsequent difference in the kinetic energy is too high. For a smoothed change of the operation mode from pulse to steady combustion (ramjet), it is recommended first to enhance the inlet area until the steady mode is almost reached

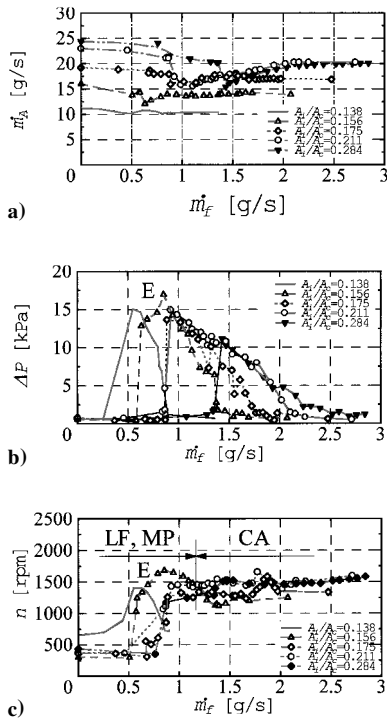


Fig. 12 Two-dimensional combustor dependency on fuel rate, with E highest efficiency and M maximum performance: a) air rate, b) amplitude, and c) turbine speed.

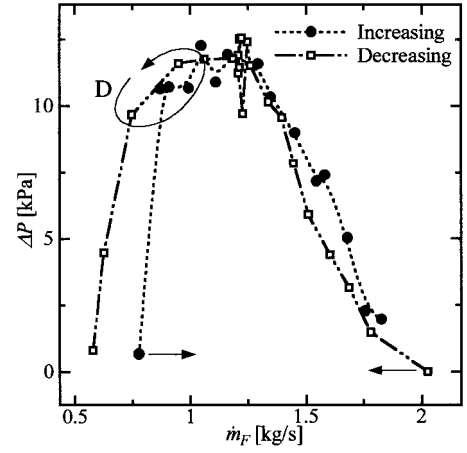


Fig. 13 Hysteresis of the pressure amplitude; arrows indicate direction for increasing and decreasing fuel rate, with D target operating range.

and then gradually to enhance the fuel rate. The energy profile is flat for higher cross sections. The propulsion can be switched to the rocket mode by closing the inlet and supplying oxygen from tanks to the combustor. Whereas the actual experiments still are used for parameter identification, it is planned for the future to realize a closed-loop control system, i.e., an automatic adjustment of the inlet cross section to the demands of the flight mission. Therefore, the dynamic behavior of a possible continuously working control system was investigated by enhancing and decreasing the fuel flow rate (CA control). A hysteresis effect in the pressure amplitude was found, as shown in Fig. 13. The reason for this hysteresis might be the flame position and the location of the combustion zone within the conical diffuser/engine that depends principally on the airflow rate and the velocity. It is not yet clear whether further benefits can be gained from an unsteady fuel supply by making use of hysteresis effects. The desired operating range is indicated by the D in Fig. 13.

Conclusions

A combined rocket, pulse-jet, and ramjet engine is preferred to propel a space plane due to considerable weight reduction and high thermal efficiency. Present experiments indicate surprisingly high fuel savings can be gained if combustors are operated in transient or pulse mode. Therefore, the transient behavior of an active control system for the combustor was investigated experimentally, and several control strategies with fuel- and airflow rate (inlet cross section) as control parameters for conventional and twin pulse combustors are proposed. The control is used not only for the change of operation mode, but also to optimize the efficiency of the pulse jet run. Hysteresis effects, possibly useful for further combustor improvement, were found. Although several details are not yet clear, the principal method of how to operate one combustor in ramjet, pulse-jet, and rocket modes was shown. It is a fact that the thrust produced by a turbojet is higher and more efficient for sustained flight at low flight velocities. Because of the short-term application of such an engine, it does not seem beneficial to select a turbojet that is used only for the takeoff.

References

- Shirouzu, M., Matsushima, K., and Nomura, S., "A Parametric Sensitivity Study on the Ascent of a SSTO," *Proceedings of the 16th International Symposium on Space Technology Science*, May 1988, pp. 1527–1534.
- Andrews, E. H., Trexler, C. A., and Emami, S., "Tests of a Fixed-Geometry Inlet-Combustor Configuration for a Hydrocarbon-Fueled Dual-Mode Scramjet," AIAA Paper 94-2817, June 1994.
- Watanabe, S., "Scramjet Nozzle Experiment with Hypersonic External Flow," *Journal of Propulsion and Power*, Vol. 9, No. 4, 1993, pp. 521–528.
- Watkins, W., and French, J., "Rocket-Based Combined Propulsion for Reusable Space Launch," *Proceedings of the 13th International Symposium*

on *Airbreathing Engines*, edited by Frederick S. Billig, AIAA, Reston, VA, 1997, pp. 1445–1455.

⁵Billig, F., and Kothari, A., “Streamline Tracing, A Technique for Designing Hypersonic Vehicles,” *Proceedings of the 13th International Symposium on Airbreathing Engines*, edited by Frederick S. Billig, AIAA, Reston, VA, 1997, pp. 997–1006.

⁶Dec, J. E., and Keller, J. O., “Time-Resolved Gas Temperatures in the Oscillating Turbulent Flow of a Pulse Combustor Tail Pipe,” *Combustion and Flame*, Vol. 80, No. 3–4, 1990, pp. 358–370.

⁷Narayanaswami, L., and Richards, G. A., “Pressure-Gain Combustion: Part I—Model Development,” *Journal of Engineering for Gas Turbines and Power*, Vol. 118, No. 3, 1996, pp. 461–467.

⁸Foa, J. V., *Elements of Flight Propulsion*, Wiley, New York, 1960, pp. 368–389.

⁹Zeutzius, M., Beylich, A. E., Matsuo, S., and Setoguchi, T., “Experi-

mental Investigation of a Gas Dynamic Thrust Vector Control,” *JSME International Journal (B)*, Vol. 39, No. 1, 1996, pp. 101–111.

¹⁰Staab, F., “Ueber Strahltriebwerke auf Grundlage des Schmidtrohres,” *Zeitschrift fuer Flugwissenschaften*, Vol. 2, No. 6, 1954, pp. 129–141 (in German).

¹¹Barr, P. K., Keller, J. O., Bramlette, T. T., and Westbrook, C. K., “Pulse Combustor Modeling—Demonstration of the Importance of Time Characteristics,” *Combustion and Flame*, Vol. 82, No. 1, 1990, pp. 252–269.

¹²Kentfield, J. A. C., and Read, M. A., “A Pressure Gain Combustor Utilizing Twin Valveless Pulsed-Combustors Operating in Antiphase,” *Proceedings of the 14th Intersociety Energy Conversion Engineering Conference*, American Chemical Society, 1979, pp. 1774–1779.

¹³Keller, J. O., and Saito, K., “Measurements of the Combusting Flow in a Pulse Combustor,” *Combustion Sciences and Technology*, Vol. 53, No. 2, 3, 1987, pp. 137–163.